

# Electronic Tuning of Thiazolyl-Capped $\pi$ -Conjugated Compounds via a Coordination/Cyclization Protocol with $B(C_6F_5)_3$

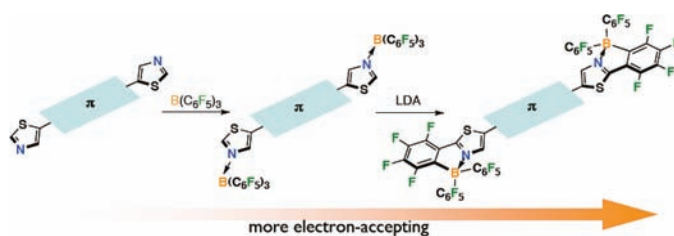
Andre Job,<sup>†</sup> Atsushi Wakamiya,<sup>\*,‡,§</sup> Gerald Kehr,<sup>†</sup> Gerhard Erker,<sup>\*,†</sup> and Shigehiro Yamaguchi<sup>\*,‡</sup>

Department of Chemistry, Graduate School of Science, Nagoya University, Furo, Chikusa, Nagoya 464-8602, Japan, and Organisch-Chemisches Institut, Universität Münster, Corrensstrasse 40, D-48149 Münster, Germany

wakamiya@scl.kyoto-u.ac.jp; erker@uni-muenster.de; yamaguchi@chem.nagoya-u.ac.jp

Received September 28, 2010

## ABSTRACT



Electronic tuning of thiazolyl-capped  $\pi$ -conjugated systems via a coordination/cyclization protocol with  $B(C_6F_5)_3$  effectively enhances an electron-accepting character giving rise to lower reduction potentials and increases thermal stability.

$\pi$ -Conjugated materials are key components for organic electronics. In their molecular designs, the crucial issues are the modification of the electronic structure at will as well as the control of the solid-state structure to gain appropriate intermolecular interactions.<sup>1</sup> In particular, the former issue is of importance to attain the required color emission, to facilitate the charge injection from the electrodes, or to achieve ambipolar carrier transport. Various methodologies for electronic tuning have been proposed. For example, Marks and co-workers demonstrated that the introduction of perfluorophenyl groups to the termini of an oligothiophene

skeleton switched its semiconducting properties from p-type to n-type.<sup>2</sup> Consequently, they succeeded in the synthesis of efficient n-type organic semiconductors for organic thin-film transistors. Recently, Bazan and co-workers also reported the electronic tuning of *N*-heteroaryl-containing  $\pi$ -conjugated skeletons based on the complexation with Lewis acids, such as  $B(C_6F_5)_3$ .<sup>3</sup> They found that this modification is effective in band gap control of the benzothiadiazole-containing conjugated oligomers.

In the molecular design of new  $\pi$ -electron materials, another important point is to employ an inherently superior skeleton. In this regard, thiazolyl-containing  $\pi$ -conjugated frameworks have several advantages as candidates for n-type

<sup>†</sup> Universität Münster.

<sup>‡</sup> Nagoya University.

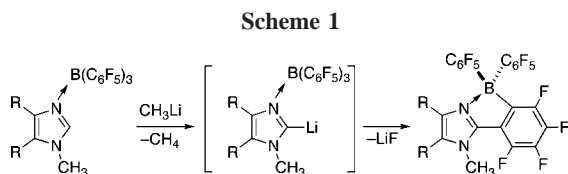
<sup>§</sup> Present address: Institute for Chemical Research, Kyoto University, Uji, Kyoto 611-0011, Japan.

(1) (a) Newman, C. R.; Frisbie, C. D.; da Silva Filho, D. A.; Brédas, J.-L.; Ewbank, P. C.; Mann, K. R. *Chem. Mater.* **2004**, *16*, 4436. (b) Kulkarni, A. P.; Tonzola, C. J.; Babel, A.; Jenekhe, S. A. *Chem. Mater.* **2004**, *16*, 4556. (c) Anthony, J. E. *Chem. Rev.* **2006**, *106*, 5028. (d) Murphy, A. R.; Fréchet, J. M. J. *Chem. Rev.* **2007**, *107*, 1066. (e) Facchetti, A. *Mater. Today* **2007**, *10*, 28.

(2) (a) Facchetti, A.; Yoon, M.-H.; Stern, C. L.; Katz, H. E.; Marks, T. J. *Angew. Chem., Int. Ed.* **2003**, *42*, 3900. (b) Yoon, M.-H.; Facchetti, A.; Stern, C. E.; Marks, T. J. *J. Am. Chem. Soc.* **2006**, *128*, 5792.

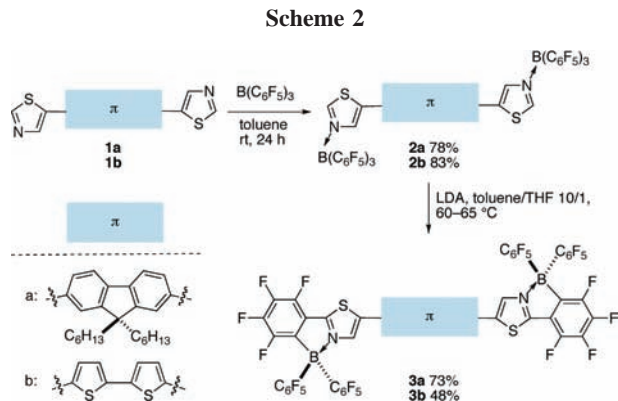
(3) Welch, G. C.; Coffin, R.; Peet, J.; Bazan, G. C. *J. Am. Chem. Soc.* **2009**, *131*, 10802.

semiconductors.<sup>4–8</sup> They exhibit relatively high electron-accepting properties, in contrast to the electron-donating thiophene analogue, facile functionalization for further modification,<sup>4</sup> and formation of close  $\pi$  stacking in the solid state.<sup>5–7</sup> For the modification of this skeleton, we now applied a reaction recently reported by the authors,<sup>9</sup> as shown in Scheme 1. The treatment of the imidazole ring with the



highly Lewis acidic borane  $B(C_6F_5)_3$  forms a B–N adduct, which is further treated with a strong base, such as methyllithium, to form a cyclized skeleton. We envisioned that the synergistic effects of the resulting intramolecular B–N coordination<sup>10,11</sup> and the extension of the  $\pi$  conjugation with the  $C_6F_4$  ring would effectively reduce the LUMO level and enhance the electron-accepting properties. We here report this “coordination/cyclization” protocol as an effective pathway to modify thiazolyl-capped  $\pi$ -conjugated skeletons.

The synthetic outline is shown in Scheme 2. As the core moiety for the thiazolyl-capped  $\pi$ -conjugated skeletons, we chose two kinds of representative skeletons, fluorene and bithiophene. Using dithiazolylfluorene **1a** and dithiazolylbithiophene **1b** as a precursor, the treatment of these compounds with  $B(C_6F_5)_3$  in toluene produced the thiazolyl– $B(C_6F_5)_3$  complexes **2a** and **2b** in good yield of 78% and 83%, respectively. Subsequently, the obtained compounds were reacted with LDA in toluene/THF (10/1) at room temperature followed by heating at 60 °C. After lithiation at the 2-position of the thiazolyl ring, the subsequent



intramolecular nucleophilic aromatic substitution at the *ortho* C–F moiety of one of the  $C_6F_5$  groups led to the cyclized products **3a** and **3b** in 73% and 48% yield, respectively. The obtained compounds **3** have good solubility in common organic solvents, such as chloroform and THF.

The thermal stability of the products was investigated by thermogravimetric analysis. While complexes **2a** and **2b** have a low decomposition temperature with a 5% weight loss ( $T_{d5}$ ) at 225 and 233 °C, respectively, both cyclized products **3a** and **3b** show high thermal stability with  $T_{d5}$  at 387 and 376 °C, respectively. These results indicate that the  $(C_6F_5)_2BC_6F_4$  cyclization significantly increases the thermal stability. We were able to sublimate **3b** around 350 °C at 0.1 mmHg to give single crystals suitable for X-ray structure analysis (Figure 1).

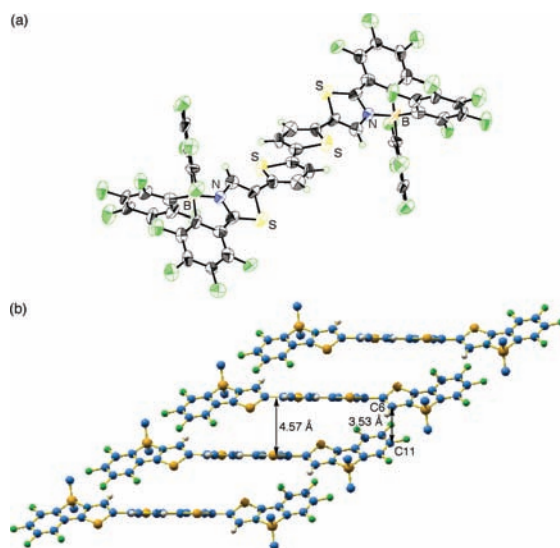


**Figure 1.** Crystal structure of **3b**: (a) ORTEP drawing with 50% probability for thermal ellipsoids and (b) packing structure (perfluorophenyl groups on the boron atom are omitted for clarity).

For gaining a large degree of electronic coupling and thus a high carrier mobility, the  $\pi$ -stacking motif with a large

- (4) (a) Jenkins, I. H.; Pickup, P. G. *Macromolecules* **1993**, *26*, 4450. (b) Ng, M.-K.; Yu, L. *Angew. Chem., Int. Ed.* **2002**, *41*, 3598. (c) Jiang, P.; Morales, G. M.; You, W.; Yu, L. *Angew. Chem., Int. Ed.* **2004**, *43*, 4471. (d) Lee, J.; Jung, B.-J.; Lee, S. K.; Lee, J.-I.; Cho, H.-J.; Shim, H.-K. *J. Polym. Sci., Part A* **2005**, *43*, 1845.
- (5) (a) Cao, J.; Kampf, J. W.; Curtis, M. D. *Chem. Mater.* **2003**, *15*, 404. (b) Cao, J.; Curtis, M. D. *Chem. Mater.* **2003**, *15*, 4424. (c) Curtis, M. D.; Cao, J.; Kampf, J. W. *J. Am. Chem. Soc.* **2004**, *126*, 4318.
- (6) Yamamoto, T.; Arai, M.; Kokubo, H.; Sasaki, S. *Macromolecules* **2003**, *36*, 7986.
- (7) (a) Ando, S.; Murakami, R.; Nishida, J.; Tada, H.; Inoue, Y.; Tokito, S.; Yamashita, Y. *J. Am. Chem. Soc.* **2005**, *127*, 14996. (b) Mamada, M.; Nishida, J.; Kumaki, D.; Tokito, S.; Yamashita, Y. *Chem. Mater.* **2007**, *19*, 5404. Yamashita, Y. *Chem. Lett.* **2009**, *38*, 870.
- (8) Hong, X. M.; Katz, H. E.; Lovinger, A. J.; Wang, B.-C.; Raghavachari, K. *Chem. Mater.* **2001**, *13*, 4686.
- (9) (a) Vagedes, D.; Kehr, G.; König, D.; Wedeking, K.; Fröhlich, R.; Erker, G.; Mück-Lichtenfeld, C.; Grimme, S. *Eur. J. Inorg. Chem.* **2002**, 2015. (b) Vagedes, D.; Erker, G.; Kehr, G.; Bergander, K.; Kataeva, O.; Fröhlich, R.; Grimme, S.; Mück-Lichtenfeld, C. *Dalton Trans.* **2003**, 1337.
- (10) Wakamiya, A.; Taniguchi, T.; Yamaguchi, S. *Angew. Chem., Int. Ed.* **2006**, *45*, 3170.
- (11) (a) Cheng, C.-C.; Yu, W.-S.; Chou, P.-T.; Peng, S.-M.; Lee G.-H.; Wu, P.-C.; Song, Y.-H.; Chi, Y. *Chem. Commun.* **2003**, 2628. (b) Klappa, J. J.; Geers, S. A.; Schmidtke, S. J.; MacManus-Spencer, L. A.; McNeill, K. *Dalton Trans.* **2004**, 883. (c) Liu, Q.-D.; Mudadu, M. S.; Thummel, R.; Tao, Y.; Wang, S. *Adv. Funct. Mater.* **2005**, *15*, 143. (d) Yoshino, J.; Kano, N.; Kawashima, T. *Chem. Commun.* **2007**, 559. (e) Zhao, Q.; Zhang, H.; Wakamiya, A.; Yamaguchi, S. *Synthesis* **2009**, 127.

overlap of  $\pi$ -orbitals with the neighboring molecules is crucial.<sup>12</sup> In the structure of **3b**, while the thiophene and thiazole ring is slightly twisted with a dihedral angle of 37°, the inner bithiophene unit and the terminal boron-bridged perfluorophenylthiazoyl units have planar conformation with dihedral angles of 0.4° and 7.3°, respectively. Overall, the dihedral angle between the central thiophene plane and the terminal C<sub>6</sub>F<sub>4</sub> ring plane is 38.9° (Figure 1a). In the packing structure, despite the bulky (C<sub>6</sub>F<sub>5</sub>)<sub>2</sub>B moiety, **3b** forms a  $\pi$ -stacked one-dimensional array (Figure 1b). The closest intramolecular distance between the thiazoyl moiety and the terminal C<sub>6</sub>F<sub>4</sub> moiety is 3.53 Å (C6··C11).

We investigated the photophysical properties of two series of compounds, **1a–3a** and **1b–3b**. Figure 2 shows the UV–vis absorption and fluorescence spectra of **1a–3a** in THF as a representative example. The data for all compounds are summarized in Table 1. Both series show a similar trend to each other. In the absorption spectra, while the complexation with B(C<sub>6</sub>F<sub>5</sub>)<sub>3</sub> only results in subtle red shifts in the absorption maximum wavelength ( $\lambda_{\text{max}}$ ), the cyclization results in significant red shifts in the  $\lambda_{\text{max}}$ , together with the significant increase of the molar absorption coefficients compared to those of **1** and **2**. In the fluorescence spectra, while the (C<sub>6</sub>F<sub>5</sub>)<sub>3</sub>B adducts **2** also show slight red shifts in the emission maxima compared to **1**, the cyclized products **3a** and **3b** show blue and yellow emissions with significantly red-shifted emission maxima by 63 and 72 nm compared to those of **2a** and **2b**, respectively. While the fluorene derivative **3a** has a smaller quantum yield than the non-modified **1a**, the bithiophene derivative **3b** maintains a comparable quantum yield with that of **1b**.

To gain deeper insight into the excited state dynamics, we measured the time-resolved fluorescence spectra. We determined the fluorescence lifetimes for all compounds and calculated the radiative ( $k_r$ ) and nonradiative ( $k_{\text{nr}}$ ) decay rate constants from the singlet excited state, based on the equations of  $k_r = \Phi_F/\tau_s$  and  $k_{\text{nr}} = (1 - \Phi_F)/\tau_s$ . Comparison of these data demonstrated that the (C<sub>6</sub>F<sub>5</sub>)<sub>3</sub>B coordination/cyclization protocol tends to slightly decrease the  $k_r$  values, whereas **1a–3a** and **1b–3b** show a different trend in the  $k_{\text{nr}}$  values from each other.

We also examined the solvent effects in the fluorescence spectra for the fluorene series **1a–3a** (Supporting Informa-

**Table 1.** Photophysical Data for **1a–3a** and **1b–3b** in THF

| compd     | absorption                       |   | fluorescence                    |            |                  |   |   |
|-----------|----------------------------------|---|---------------------------------|------------|------------------|---|---|
|           | $\lambda_{\text{abs}}^a$<br>[nm] | $\epsilon$<br>[M <sup>-1</sup> cm <sup>-1</sup> ] | $\lambda_{\text{em}}^b$<br>[nm] | $\Phi_F^c$ | $\tau_s$<br>[ns] | $k_r$<br>[10 <sup>8</sup> s <sup>-1</sup> ] | $k_{\text{nr}}$<br>[10 <sup>8</sup> s <sup>-1</sup> ] |
| <b>1a</b> | 346                              | 48200   | 375                             | 0.82       | 1.2              | 6.8   | 1.5   |
| <b>2a</b> | 352                              | 46900   | 413                             | 0.56       | 1.1              | 5.1   | 4.0   |
| <b>3a</b> | 399                              | 59700   | 476                             | 0.40       | 1.0              | 4.0   | 6.0   |
| <b>1b</b> | 381                              | 32500   | 442                             | 0.18       | 0.48             | 3.8   | 17.1  |
| <b>2b</b> | 388                              | 33200   | 476                             | 0.13       | 0.52             | 2.5   | 16.7  |
| <b>3b</b> | 432                              | 41400   | 548                             | 0.15       | 0.89             | 1.6   | 9.5   |

<sup>a</sup> Only the longest absorption maxima are shown. <sup>b</sup> Emission maxima upon excitation at the absorption maximum wavelengths. <sup>c</sup> Absolute quantum yield determined by a calibrated integrating sphere system (within errors of  $\pm 3\%$ ).

tion). While the parent compound **1a** shows almost no change both in absorption and fluorescence spectra, (C<sub>6</sub>F<sub>5</sub>)<sub>3</sub>B-coordinated and (C<sub>6</sub>F<sub>5</sub>)<sub>2</sub>BC<sub>6</sub>F<sub>4</sub>-cyclized derivatives **2a** and **3a** show red shifts in the fluorescence spectra with increasing polarity of the solvent. According to the Lippert–Mataga plot,<sup>13</sup> the dipole moment changes from the ground state to the excited state are 19.6 and 20.3 D for **2a** and **3a**, respectively. These results demonstrated that both the (C<sub>6</sub>F<sub>5</sub>)<sub>3</sub>B coordination and (C<sub>6</sub>F<sub>5</sub>)<sub>2</sub>BC<sub>6</sub>F<sub>4</sub> cyclization enhance the intramolecular charge transfer character in the excited state to a comparable extent.

To elucidate the electronic effects of the present modifications on the photophysical properties, DFT calculations were conducted on model compounds **1a'–3a'**, which are 9,9-dimethylfluorene derivatives of **1a–3a** (Figure 3). According to the TD-DFT calculations, the observed longest absorption bands in **1a–3a** are assignable to the  $\pi$ – $\pi^*$  transitions. In the parent compound **1a'**, the Kohn–Sham (KS) HOMO and LUMO are delocalized over the whole  $\pi$  skeleton with the potentials of  $-5.62$  and  $-1.78$  eV, respectively. The (C<sub>6</sub>F<sub>5</sub>)<sub>3</sub>B coordination in **2a'** decreases not only the LUMO level by  $-1.10$  eV but also the HOMO level to a similar extent. As a result, the transition energies for **1a'** and **2a'** are comparable to each other, despite the significant differences in the HOMO and LUMO energy levels. In contrast, in **3a'**, while the (C<sub>6</sub>F<sub>5</sub>)<sub>2</sub>BC<sub>6</sub>F<sub>4</sub> cyclization further decreases the LUMO level, the HOMO level is increased due to the extension of the  $\pi$  conjugation with the additional C<sub>6</sub>F<sub>4</sub> rings. Consequently, compound **3a** shows the significantly red-shifted absorption band. This coordination/cyclization protocol also makes the  $\pi$  orbital and  $\pi^*$  orbital more localized on the inner fluorene  $\pi$ -conjugated moiety and the terminal B–N-coordinated thiazole moieties, respectively. This increases a

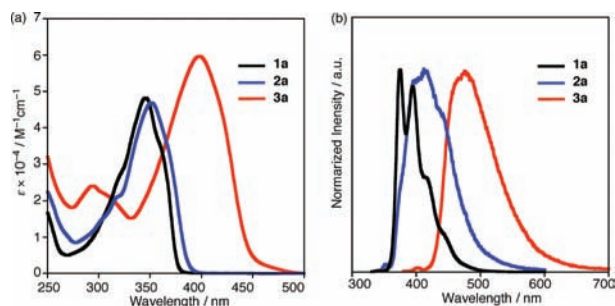


**Figure 2.** Photophysical properties of **1a–3a**: (a) absorption and (b) fluorescence spectra in THF.

(12) (a) Cornil, J.; Beljonne, D.; Calbert, J.-P.; Brédas, J.-L. *Adv. Mater.* **2001**, *13*, 1053. (b) Kim, E.-G.; Coropceanu, V.; Gruhn, N. E.; Sánchez-Carrera, R. S.; Snoberger, R.; Matzger, A. J.; Bédas, J.-L. *J. Am. Chem. Soc.* **2007**, *129*, 13072.

(13) Although the Lippert–Mataga equation originally assumes the presence of a molecular dipole, it has been demonstrated to be applicable to several quadrupole extended  $\pi$ -conjugated molecules. See: (a) Strehmel, B.; Sarker, A. M.; Malpert, J. H.; Strehmel, V.; Seifert, H.; Neckers, D. C. *J. Am. Chem. Soc.* **1999**, *121*, 1226. (b) Krebs, F. C.; Spanggaard, H. *J. Org. Chem.* **2002**, *67*, 7185. (c) Zhao, C.-H.; Sakuda, E.; Wakamiya, A.; Yamaguchi, S. *Chem.–Eur. J.* **2009**, *15*, 10603.

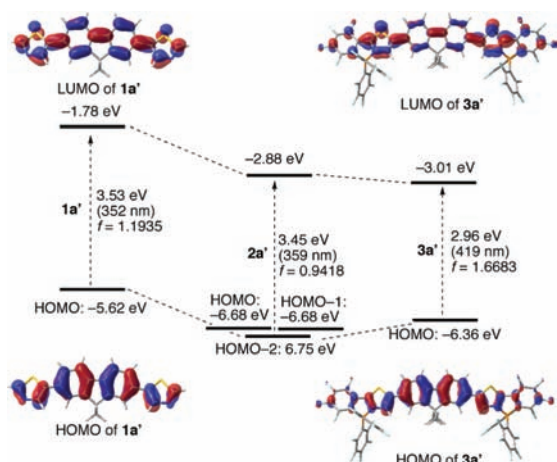


**Figure 3.** Plot of the Kohn–Sham HOMO and LUMO energy levels for **1a'**–**3a'** and pictorial presentations of HOMOs and LUMOs of **1a'** and **3a'**. The  $\pi$ – $\pi^*$  transition energies and oscillator strengths are calculated by TD DFT at the B3LYP/6-31G(d) level.

quadrupolar acceptor–donor–acceptor character, resulting in the more significant intramolecular charge transfer character in the excited state in **2a** and **3a**.

How the present modifications affect the electrochemical properties is also an important issue in this chemistry. We carried out the measurements of cyclic voltammetry in THF to determine the reduction potentials (Figure 4). While the parent compounds **1a** and **1b** only show irreversible reduction waves with the peak potentials ( $E_{pc}$ ) at  $-2.86$  and  $-2.44$  V (vs a ferrocene/ferrocenium couple), respectively, the  $(C_6F_5)_2BC_6F_4$ -cyclized **3a** and **3b** show two-step reduction waves at more positive potentials  $E_{pc} = -1.81$  V ( $E_{1/2} = -1.74$  V) and  $-1.96$  V for **3a** and  $-1.70$  V ( $E_{1/2} = -1.61$  V) and  $-1.89$  V for **3b**, with increased reversibility for the first reduction waves. These results well demonstrate the effect of the  $(C_6F_5)_2BC_6F_4$  cyclization for lowering the LUMO level. On the basis of the observed first reduction potentials, the LUMO levels of **3a** and **3b** are estimated to be 3.1 and 3.2 eV, respectively.<sup>14</sup> These values are sufficiently low to facilitate electron injection from the cathode in electron-transporting devices.<sup>1a,b</sup> For the  $(C_6F_5)_3B$ -coordinated **2a** and **2b**, we observed only irreversible reduction waves around  $-2.3$  and  $-2.1$  V, respectively, indicating their instability under the measurement condition. These results demonstrate that the  $(C_6F_5)_2BC_6F_4$ -cyclized

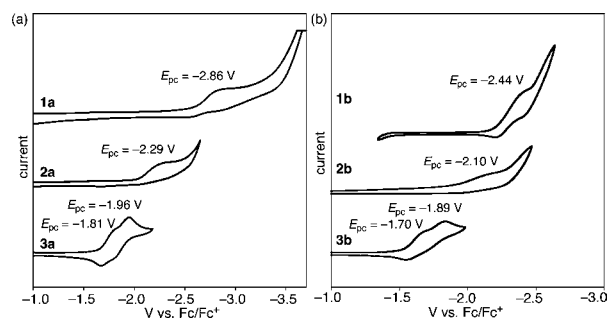


**Figure 4.** Cyclic voltammograms of (a) **1a**–**3a** and (b) **1b**–**3b** in THF, measured with  $[n\text{-Bu}_4\text{N}][\text{PF}_6]$  (0.1 M) as a supporting electrolyte at a scan rate of  $100$  mV s<sup>-1</sup>.

structure is also effective in stabilizing the produced anionic species.

In summary, we have demonstrated that the  $(C_6F_5)_3B$  coordination/cyclization protocol is effective for tuning the electronic structure of thiazoyl-capped  $\pi$ -conjugated compounds. The electron affinity can be increased by the  $(C_6F_5)_2BC_6F_4$  cyclization. This modification also endows charge transfer character in their photophysical properties. It is also worth noting that  $(C_6F_5)_2BC_6F_4$  cyclization is effective for increasing the thermal stability. Further study of the development of new n-type semiconducting materials using this protocol is now in progress.

**Acknowledgment.** This work was supported by the IRTG program of Münster University–Nagoya University and Grants-in-Aid (No. 19685004 and 19675001) from the Ministry of Education, Culture, Sports, Science, and Technology, Japan.

**Supporting Information Available:** Experimental details, thermogravimetric analysis, photophysical data, results of theoretical calculations, and crystallographic data in CIF format. These materials are available free of charge via the Internet at <http://pubs.acs.org>.

OL102282X

(14) Pommerehne, J.; Vestweber, H.; Guss, W.; Mahrt, R. F.; Bäessler, H.; Porsch, M.; Daub, J. *Adv. Mater.* **1995**, *7*, 551. The LUMO levels were estimated based on the fact that the reduction potential ( $E_{1/2}$ ) of ferrocene corresponds to 4.80 eV.